

1928 + 738: A SUPERLUMINAL SOURCE WITH LARGE-SCALE STRUCTURE

K. J. JOHNSTON AND R. S. SIMON

E. O. Hulburt Center for Space Research, Naval Research Laboratory

A. ECKART, P. BIERMANN, C. SCHALINSKI, AND A. WITZEL

Max-Planck-Institut für Radioastronomie

AND

R. G. STROM

Netherlands Foundation for Radio Astronomy

Received 1986 September 11; accepted 1986 November 12

ABSTRACT

The quasar 1928 + 738 has been mapped with resolutions of $1''.2$ and $30''$ at 20 and 49 cm wavelengths, respectively, and displays two-sided radio structure which extends up to $40''$ on either side of the compact core along a position angle close to 0° . The redshift of this object (0.3) would indicate that the overall linear size of this emission is $235 h^{-1}$ kpc ($H_0 = 100 h$ km s $^{-1}$ Mpc $^{-1}$, $q_0 = 0.05$). The core of this radio source has been reported to display apparent superluminal motion which suggests that the small-scale structure is aligned within 12.5° of the line of sight to the source. If the large-scale structure is also aligned at this angle, the deprojected size is approximately $800 h^{-1}$ kpc. As this is unlikely, the large-scale structure is probably aligned to the line of sight at a considerably different angle ($> 24^\circ$) than that predicted by the superluminal motion of the milliarcsecond structure. Comparison of the large-scale structure of 1928 + 738 with other superluminal sources indicates that large-scale symmetrical structure with two large radio lobes placed on either side of the compact emission is a common phenomenon among these objects. 1928 + 738 is unique among superluminal sources in having jetlike emission symmetrically placed about the compact core.

Subject headings: radio sources: extended — radio sources: general — radio sources: variable

I. INTRODUCTION

Extragalactic radio sources appear to fall into two varieties, those which display large-scale symmetrical structure with two large radio lobes placed on either side of a compact radio source, and those with one-sided asymmetrical structure. The latter are thought to be seen typically in those sources displaying apparent superluminal motion. For the latter sources, the structure does not appear to be very large, and this asymmetry is ascribed to the alignment of the radio source axis close to the line of sight. The mapping of the arcsecond scale structure of superluminal sources with high dynamic range may detect the large-scale radio lobes if this supposition is correct. The arcsecond structure of superluminal radio sources is described by Browne *et al.* (1982); Browne and Orr (1981); Perley, Fomalont, and Johnston (1982); and Schilizzi and de Bruyn (1983). The object 3C 273 displays one-sided arcsecond scale emission, while 3C 120, 3C 179, 3C 279, 3C 345, 3C 395, NRAO 140, 1642 + 690, and BL Lac have complex emission on arcsecond scales.

Recently apparent superluminal motion was detected in the quasar 1928 + 738 (Eckart *et al.* 1985). Here we report the detailed large-scale radio emission from this source at wavelengths of 20 and 49 cm.

II. OBSERVATIONS

The VLA¹ in the A configuration was used in 1983 October 31 at a wavelength of 20 cm. The observations were conducted over a 12 hr period. These observations were interspersed with observations of 1803 + 784. The complete details of these observations, together with a description of the detailed radio structure of the S5 sources described in Eckart *et al.* (1986*a*, *b*) are to be the subject of a future paper. The flux density scale was established by assuming that 3C 286 has a flux density of 14.71 Jy at 20 cm (Baars *et al.* 1977).

The data were initially calibrated by assuming that 1803 + 784 was unresolved and could be used as a phase and amplitude reference to correct the individual antenna gains for the observations of 1928 + 738. Images made from this initial calibration, even after several iterations of self-calibration (e.g., see Pearson and Readhead 1984 and references therein) showed low-level systematic image defects in the form of radial striations and ringlike halos which suggested that residual calibration errors remained in the map;

¹The Very Large Array (VLA) is run by the National Radio Astronomy Observatory which is operated by Associated Universities, Inc., under contract with the National Science Foundation.

similar errors also occurred in a map of 1803+784. The rms noise level in the map was also much higher than the expected thermal noise which again suggested that the signal-to-noise ratio level in the map was dominated by calibration errors which self-calibration had not been able to remove. The ratio of the peak brightness in this initial image to the rms noise level was $\sim 2000:1$, so that many of the features in our final map were hidden by the artificially high noise level. A further indication of residual calibration errors was that summing the images made independently from the two 50 MHz VLA channels did not improve either the noise level in the map or significantly reduce the low-level image defects.

Since 1928+738 had been observed with extremely good (u, v) plane sampling, we attempted to correct for baseline-dependent (closure) errors in the data using the baseline by baseline algorithm called BCAL in AIPS. BCAL finds a correction for the complex gain on each baseline by assuming an input model of the source is correct and adjusts each baseline gain so that the average difference between the observed visibility and the model visibility is zero. In order for BCAL to succeed, there MUST be sufficient sampling of the (u, v) plane so that many (u, v) cells are overdetermined, or simply that many of the (u, v) plane tracks intersect. This is the case for sources like 1928+738 observed with long tracks on the VLA, but is not the case for "snapshot" observations. If there is greatly insufficient sampling, the map made from data processed by BCAL will bear a strong resemblance to the input model but with the noise level artificially reduced. Even with long tracks in the (u, v) plane, errors can be introduced in the final map if there are not enough crossing points of projected baseline tracks. This sort of error will show up as a strange tapering of the (u, v) plane data and hence an unusual convolution could be applied to the image. Again, the output map will bear a strong resemblance to the input map with the noise level artificially reduced.

To use BCAL for 1928+738, we initially attempted using the first map described above as our input model. This was only a partial success, since a number of the image defects were included in the input map. The resulting map from this initial BCAL was improved, in that the weak emission to the north was just discernible, but there were still radial artifacts in the map, the noise level was still high, and one of the two 50 MHz maps was noticeably better than the other. Iterating BCAL with this image produced no improvement; the map artifacts had been "frozen" into the model.

As an experiment, we tried using a point source model for the initial input map to BCAL. This was, in effect, an unbiased way to ignore all the errors introduced into the source model by calibration errors. It worked spectacularly well for 1928+738 because it is heavily dominated by the unresolved core. All of the faint low-brightness emission which had been suspected from the earlier mapping attempts now showed up clearly, even though it had not been introduced as part of the starting model. In addition, the two independent 50 MHz channels now produced similar maps, with a dramatically improved noise level. We iterated BCAL until a stable source model was achieved. The two channels were mapped independently in this fashion and then compared to help ensure that

artifacts were not introduced; there was essentially no difference in either the noise level or the features seen in the two images. Our final image is the average of the two images.

BCAL was thus able to eliminate closure errors from our input data which ordinary calibration techniques could not. We emphasize that this was possible because of our extensive (u, v) plane coverage and because 1928+738 is heavily dominated by an unresolved core. The rms corrections for each baseline were $\sim 1\%$.

A CLEANed map displaying all the structure of 1928+738 is shown in Figure 1a. The cell size is $0''.2$. Natural weighting was applied to the uv data. The restoring beam was $1''.8$ by $1''.6$ along a position angle of $61^\circ 8'$. The peak brightness is 3.350 Jy per beam while the total flux density is 3.548 Jy. The number of clean components was 4000. This map contains two streams of emission extending out from the central source. The southern emission appears to bend from about -170° to 160° . The northern emission appears to end in a large amorphous region of about $15''$ in diameter. The dynamic range of this map, defined as the ratio of the peak brightness to the RMS noise level, is of order 24,000:1.

A higher resolution CLEANed map is shown in Figure 2a. This map was made in a fashion similar to the previous one except that the uv data plane was uniformly tapered and only 400 components were restored. The restoring beam is $1''.2$ by $1''.1$ along a position angle of -54° . The innermost source south of the compact emission is shown to be resolved from the compact emission. In addition, the emission in all the features is unresolved perpendicular to the longer axis of the component with the exception of the northernmost amorphous component. The major components are listed in Table 1. The flux densities were taken from the map in Figure 1a with the exception of component 2 for which the map of Figure 2 was used. The positions are from the map of Figure 2 and refer to the peak brightness for each component, except the position of component 7 is from its approximate center on the map in Figure 1a. The total flux density of the seven components, 3.526 Jy, is almost equal to the total cleaned flux density of 3.548 Jy.

The Westerbork Synthesis Radio Telescope (WSRT)² was used in its high dynamic range redundancy mode at 49 cm in 1982 December. Both redundancy corrections and a self-calibration-type procedure were employed (Noordam and de Bruyn 1982) to obtain a dynamic range exceeding 1000:1. At this level and with the WSRT resolution of $30''$, 1928+738 consists of three components: a dominant central source, and a weak double structure elongated by about $36''$ in a nearly north-south direction. Flux densities for the three components based upon the self-calibration model fitting are given in Table 1. A map of the double structure after subtraction of the nuclear component is shown in Figure 1b. (Because only one polarization configuration was used, the map is of the Stokes parameters $I + Q$.) There is evidence that the southern component is significantly resolved, and that the emission to the west is extended. While the northern lobe corresponds

²The Westerbork Synthesis Radio Telescope is operated by the Netherlands Foundation for Radio Astronomy with the financial support of the Organization for the Advancement of Pure Research (ZWO).

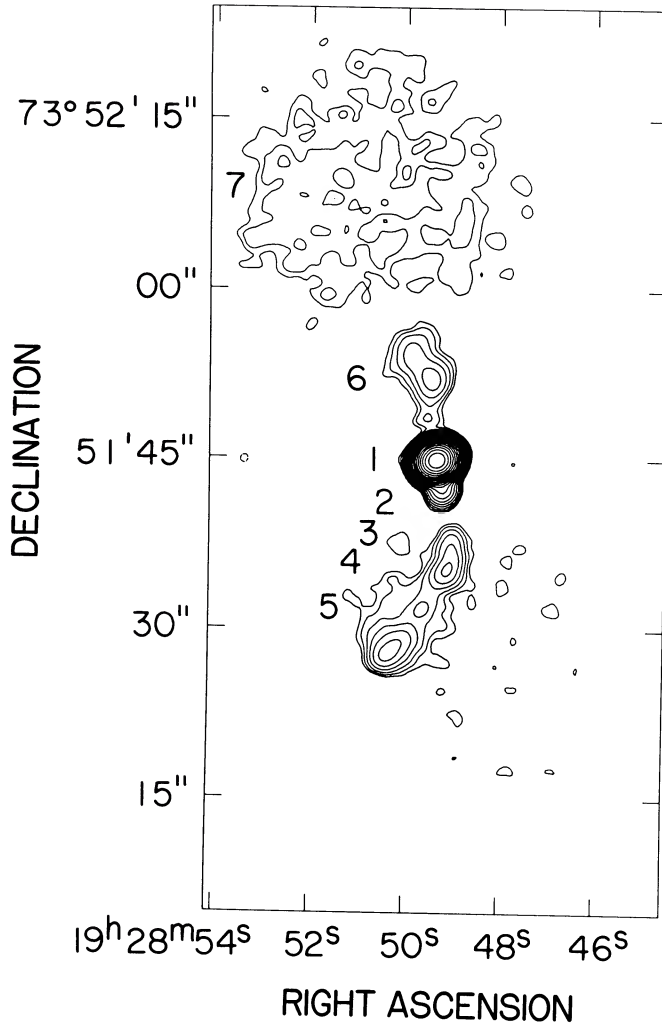


FIG. 1a

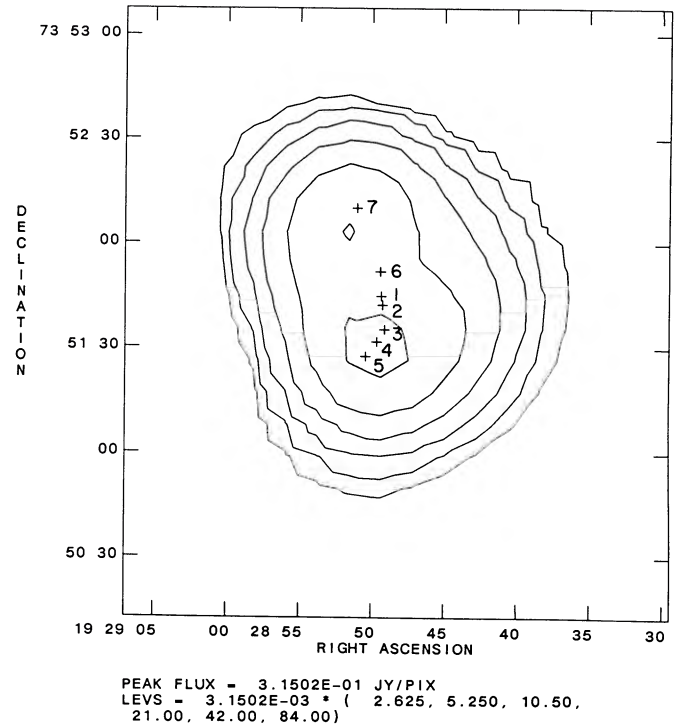


FIG. 1b

FIG. 1.—(a) A map of 1928 + 738 at 20 cm wavelength. The cell size was $0''.2$. This map was restored with a $1''.6$ by $1''.6$, $\text{pa } -62^\circ$ Gaussian beam. The emission is seen to be distributed in either side of the compact emission which had a flux density of 3.350 Jy per beam. The contour levels are 0.00053, 0.00084, 0.0013, 0.0021, 0.0034, 0.0053, 0.0084, 0.013, 0.021, 0.034, 0.053, 0.084, 0.133, 0.211, 0.335, 0.531, 0.842, 1.223, and 2.114 Jy per beam. These levels correspond to contour intervals of 2 db, with contours from -2 db down to -38 db down from the peak map brightness. This map has a dynamic range of 24,000:1. (b) The brightness distribution at 20 cm of 1928 + 738 after subtraction of the dominant central component. Contours have been drawn at levels of 8.3, 16.5, 33.1, 66.2, 132.3, and 264.6 mJy per beam. The lowest contour is about 0.2% of the peak brightness in the original map. (Crosses indicate the positions of components found in the VLA map.)

to components 6 and 7 of Figure 1a, the southern one must largely be resolved out in the VLA map, because components 3, 4, and 5 supply only a fraction of its total flux density at 20 cm and the spectral index of this southern component is -2.4 if *all* the flux density is accounted for in the 20 cm maps. Therefore, -2.4 is simply a lower limit to the spectral index for the southern component.

This comparison of the 20 and 49 cm maps indicates that there may be amorphous extended emission southwest of component 5 that is not seen on the 20 cm map.

III. DISCUSSION

The redshift of this quasar was recently determined to be 0.302 (Lawrence *et al.* 1986). Deconvolving the contours in

Figure 1b with a $30''$ beam shows the emission to be spread out over about $80''$. At the given redshift, $1''$ corresponds to $2.94 h^{-1}$ kpc ($H_0 = 100 h \text{ km s}^{-1} \text{ Mpc}^{-1}$, $q_0 = 0.05$ is assumed throughout this Letter). The linear size of this emission is therefore $235 h^{-1}$ kpc. The standard model for apparent superluminal motion is that of relativistic motion in a jet pointed nearly along the line of sight (Blandford and Königl 1979). If we believe that the large-scale radio emission is also beamed at us and is at the same angle with the line of sight as the compact emission ($< 12^\circ$), the deprojected length is of order $1 h^{-1}$ Mpc. In deprojecting the source, one must account for the radio lobes. The size of the radio lobes is independent of viewing angle and will reduce the deprojected size by an estimated 20%. This would make this source one of the largest known quasars. There are two possible explana-

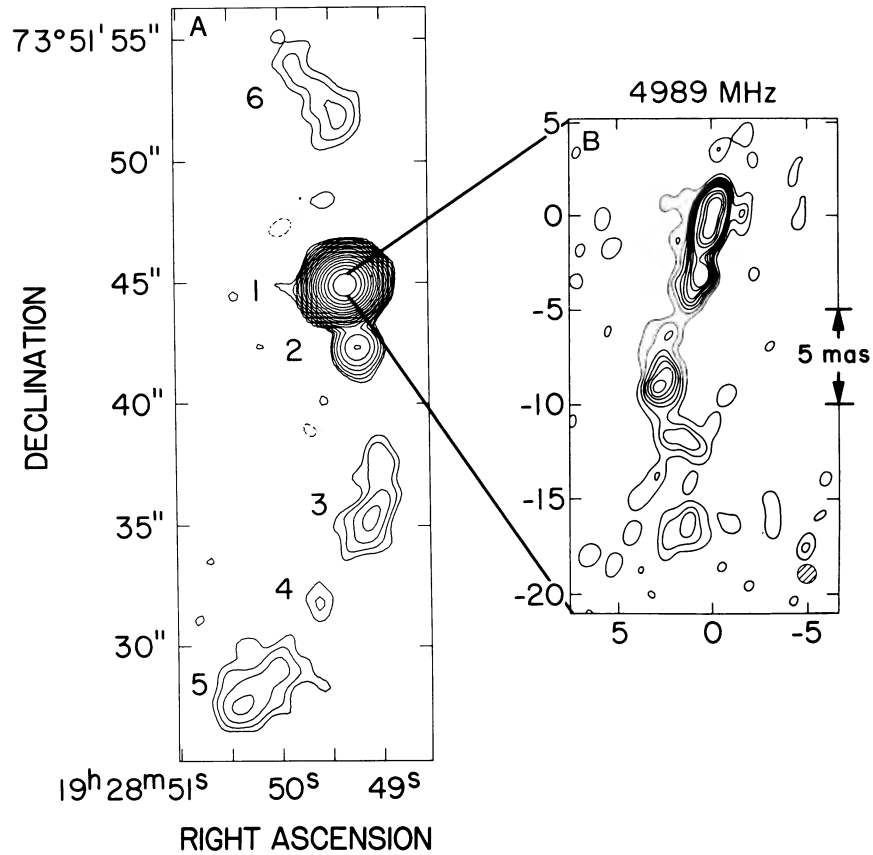


FIG. 2.—(a) A full-resolution 20 cm wavelength map made with uniformly weighted uv data. The restoring beam is $1''.2$ by $1''.1$, $pa -54^\circ$. Note that all components are unresolved perpendicular to their longer axis. The amorphous northern component did not appear well on the map so it was not plotted. The peak flux density is 3.349 Jy per beam. The contour levels are $-0.00084, 0.00084, 0.0012, 0.0021, 0.0033, 0.0053, 0.0084, 0.013, 0.021, 0.033, 0.053, 0.084, 0.122, 0.211, 0.335, 0.531, 0.841, 1.334,$ and 2.114 Jy. (b) The milliarcsecond resolution 6 cm map of 1928+738 from Eckart *et al.* (1985). There are at least nine components.

TABLE 1
COMPONENTS OF 1928+738

COMPONENT	R.A. (1950)	DECL.(1950)	20 CENTIMETER		49 CENTIMETER		α_{49}^{20}
			Peak Flux Density (Jy per beam)	Total Flux Density (Jy)	Total Flux Density (Jy)		
1	19 ^h 28 ^m 49 ^s .347	+73°51'44".90	3.350	3.350	4.5	-0.3	
2	19 28 49.251	73 51 41.30	0.016	0.016			
3	19 28 49.108	73 51 35.30	0.006	0.016	0.32	> -2.4	
4	19 28 49.635	73 51 31.70	0.003	0.005			
5	19 28 50.403	73 51 27.50	0.007	0.019			
6	19 28 49.395	73 51 51.90	0.002	0.009	0.2	-0.6	
7	19 28 51.0	73 52 10.0		0.111			
Total component flux density				3.526			
Total cleaned component flux density				3.548			

tions: 1928 + 738 is $\sim 800 h^{-1}$ kpc in size, or the arcsecond emission is nearly in the plane of the sky and is misaligned with the angle predicted by the superluminal motion of the compact core.

Typical sizes of quasar emission can be evaluated as follows. The apparent size of the emission for 3C 120 and 1928 + 738 is typical of large-scale structure found from a complete sample of 4C radio sources in the 20° – 40° declination strip (Olsen 1970; Schmidt 1974). Wardle and Potash (1984) mapped the eight largest angular size ($> 50''$) quasars of a total of 32 that clearly have resolved double or triple structure in this sample. The apparent major axes of these quasars vary from 200 to $400 h^{-1}$ kpc. The angle between the line of sight and the major axes of these quasars may be estimated to be between 76° and 90° ($76^\circ = \cos^{-1}\{8/32\}$). These sources display two-sided emission with one side dominant. No counterjet is displayed in any of the eight sources. Similar size scales (100 – $350 h^{-1}$ kpc) were also found for the major axis of Fanaroff and Riley (1974) class II sources (high-luminosity, edge-brightened “classical doubles”) by Burns *et al.* (1984). This would appear to indicate that typical sizes for large quasars are in the range 150 – $300 h^{-1}$ kpc. Therefore the size of 1928 + 738 is probably of order $300 h^{-1}$ kpc and the large-scale emission is aligned at a larger angle with respect to the line of sight than that predicted by superluminal motion. If one accounts for the radio lobes, this angle with the line of sight does not have to be very large. An angle of 24° would indicate a size of order $400 h^{-1}$ kpc. However, a size of $800 h^{-1}$ kpc cannot be ruled out as the major axis of the quasar 4C 34.47 is $1 h^{-1}$ Mpc (Conway, Burn, and Vallee 1977; Jagers *et al.* 1982). Radio galaxies have been found which are as large as $4 h^{-1}$ Mpc (3C 236; Strom and Willis 1980).

The milliarcsecond scale radio emission is shown in Figure 2*b* (Eckart *et al.* 1985). Inspection of Figure 2*a* shows that

the emission is nearly continuous on the side that displays apparent superluminal motion. This may be used as an indirect argument that the velocity of the jet is continuous out to kpc distances from the core. Again for all superluminal sources the arcsecond scale emission closest to the compact core is more dominant in the same direction as the milliarcsecond structure. The emission from 1928 + 738 seems to be corkscrew in shape on the milliarcsecond scale. However on arcsecond scales this emission bends in one direction. As pointed out by Schilizzi and de Bruyn (1983) for other superluminal sources, the arcsecond structure may be misaligned to the milliarcsecond structure due to a precession or wobble of the beam. Thus the milliarcsecond structure may be viewed at a much different angle to the line of sight than the arcsecond structure.

1928 + 738 also appears to display a counterjet. This phenomenon is not ordinarily seen in powerful radio sources; 1928 + 738 is the only superluminal source which has jetlike emission on either side of the compact core. The superluminal sources 3C 179 (Porcas 1984), 3C 120 (Walker 1984), 3C 395 (Perley, Fomalont, and Johnston 1982) 3C 345, NRAO 140, BL Lac (Schilizzi and de Bruyn 1983), 1642 + 690 (Browne and Orr 1981), 3C 279 (Ulvestad *et al.* 1981), and 1928 + 738 display emission on both sides of the compact core. Large extended radio lobes are evident in 3C 179, 3C 120, 3C 279, and NRAO 140. The emission from BL Lac appears to be complex and is at a low level. A summary of the morphology and size of the emission is given in Table 2. All of the objects are quasars with the exception of 3C 120 which is a radio galaxy. Thus among the known apparent superluminal sources (3C 273, in addition to the those already mentioned), there are nine of 10 that display emission on either side of the compact superluminal source. The unprojected size of this emission varies from 4 to $235 h^{-1}$ kpc. Two of the sources (3C 120 and 1928 + 738) have apparent major axes in the

TABLE 2
MORPHOLOGY AND SIZE OF SUPERLUMINAL SOURCES

Source	Morphology ^a	z	Size	v/c	θ max ^b	Minimum Apparent Size (h^{-1} kpc)	Deprojected Size ^c (h^{-1} kpc)	References
3120	D	0.033	360''	2.1	51°	165	212	1
NRAO 140.....	D	1.258	11	5.4	21	61	170	
3C 179	C/D	0.846	16	4.2	27	80	176	
3C 273	A	0.158	20	5.3	21	36	100	1
3C 279	C/D	0.538	18	3.5	32	74	140	1
3C 345	D	0.595	20	8.2	3	85	1620	1, 2, 3
1642 + 690	D	0.75	11	9.3	12.3	53	249	4, 5
1928 + 738	D	0.302	80	9.1	12.5	235	1090	6, 7
3C 395	D	0.635	1	10.5	10.9	4	21	8, 9, 10
BL Lac.....	C	0.07	25	2.0	53	22	28	2, 3

^aA = asymmetric; C = complex; D = double.

^bAssumes that large-scale emission is misaligned to the line of sight by the angle predicted by the apparent superluminal motion.

^c θ max is derived from $\theta_{\max} = 2 \cot^{-1}(v/c)$ for all sources except 3C 345 for which additional constraints are available (Cohen and Unwin 1984). If v/c were the only constraint, $\theta_{\max} = 14$ for 3C 345 and the deprojected size is only $> 351 h^{-1}$ kpc.

REFERENCES.—(1) Browne *et al.* 1982. (2) Cohen and Unwin 1984. (3) Schilizzi and de Bruyn 1983. (4) Pearson *et al.* 1986. (5) Browne and Orr 1981. (6) Eckart *et al.* 1985. (7) This paper. (8) Waak *et al.* 1985. (9) Perley *et al.* 1982. (10) Simon *et al.* 1987.

range of the large quasars observed by Wardle and Potash (1984).

Table 2 also contains the deprojected size of the source assuming it is aligned with the line of sight along the angle given by the apparent superluminal motion. The quasar with the largest size is 3C 345. This source has the smallest angle to the line of sight: 3° . Inspection of the large quasars mapped by Wardle and Potash (1984) shows that the ratio of the major axis of the quasar to the width of the lobes varies from 10 to 5. Thus, quasars with these ratios would display a linear size equal to the size of the radio lobes at angles to the line of sight of less than 6° – 12° . This is probably the case for 3C 345. Its deprojected size may be in the range 400 – $800 h^{-1}$ kpc. The angles for the other objects are greater than 12° . However, here again, the radio lobes will again cause large overestimates of the sizes of the sources. The deprojected sizes are only poor upper limits to their sizes. The deprojected size of all superluminal sources shows that the major axis of 1928 + 738 is very large compared with the other sources. The deprojected sizes for four of the 10 sources are found to be larger than 200 kpc. This is unlikely. This may be taken as evidence that the large-scale emission is usually not aligned with the compact emission. Bending of radio emission from the core to the outer radio lobes is a common phenomenon among extragalactic radio sources.

An alternate explanation is that the milliarcsecond emission observed may be a "sidelobe" of the jet. In this scenario the compact and large-scale emission are along the same axis which is at a large angle with respect to the line of sight. This "sidelobe" is then along a small angle to the line of sight and is Doppler-boosted so that its emission appears to greatly

exceed that of the milliarcsecond jet. It is usually seen in the same direction as the large-scale emission as this is the direction of the jet with which the sidelobe is aligned. This would predict that apparent superluminal motion is a very common phenomenon in quasars. This has yet to be confirmed because of the difficulty of making high angular resolution measurements, but with the advent of the VLBA, this prediction can be tested. Of the two explanations, the second explanation, i.e., that the compact core emission and the large-scale structure are not aligned, seems most likely, although the other explanations cannot be ruled out.

IV. CONCLUSIONS

The radio emission from the quasar 1928 + 738 has been shown to extend over $80''$ at wavelengths of 20 and 49 cm. This emission is found centered on the compact radio source. The emission is continuous out to kpc scales in the direction of the milliarcsecond emission. The apparent overall size of the emission is $235 h^{-1}$ kpc. If the source is oriented along the line of sight ($< 12.5^\circ$) as indicated by the apparent superluminal motion, its size would be of order $800 h^{-1}$ kpc. Therefore the large-scale structure is probably not aligned to the line of sight as is the milliarcsecond scale emission, but at a slightly larger angle of $> 24^\circ$ or the simple explanation for superluminal motion must be modified. Comparison of the large-scale radio structure of 1928 + 738 with other superluminal sources indicates that large-scale radio structure is probably as common among apparent superluminal sources as it is in radio quasars. The apparent size of their large-scale emission is typical of other quasars.

REFERENCES

- Baars, J. W. M., Genzel, R., Pauliny-Toth, I. I. K., and Witzel, A. 1977, *Astr. Ap.*, **61**, 99.
- Blandford, R. D., and Königl, A. 1979, *Ap. J.*, **232**, 34.
- Browne, I. W. A., Clark, R. R., Moore, P. K., Muxlow, T. W. B., Wilkinson, P. N., Cohen, M. H., and Porcas, R. W. 1982, *Nature*, **299**, 788.
- Browne, I. W. A., and Orr, M. J. L. 1981, in *Optical Jets in Galaxies* (ESA SP-162) (Paris: European Space Agency), p. 87.
- Burns, J. O., Basart, J. P., de Young, D. S., and Ghiglia, D. C. 1984, *Ap. J.*, **283**, 515.
- Cohen, M. H., and Unwin, S. C. 1984, in *IAU Symposium 110, VLBI and Compact Radio Sources*, ed. R. Fanti, K. Kellermann, and G. Setti (Dordrecht: Reidel), p. 95.
- Conway, R. G., Burn, B. J., and Vallee, J. P. 1977, *Astr. Ap. Suppl.*, **27**, 155.
- de Vegt, Ch., Schramm, J., and Johnston, K. J. 1986, *A. J.*, in press.
- Eckart, A., Schalinski, C., Witzel, A., Biermann, P., Johnston, K. J., and Simon, R. S. 1986a, *Astr. Ap.*, **168**, 17.
- _____. 1986b, *Astr. Ap. Suppl.*, in press.
- Eckart, A., Witzel, A., Biermann, P., Pearson, T. J., Readhead, A. C. S., and Johnston, K. J. 1985, *Ap. J. (Letters)*, **296**, L23.
- Fanaroff, B. L., and Riley, J. M. 1974, *M.N.R.A.S.*, **167**, 31P.
- Jagers, W. J., van Brugel, W. J. M., Miley, G. K., Schilizzi, R. T., and Conway, R. G. 1982, *Astr. Ap.*, **105**, 278.
- Lawrence, C. R., Pearson, T. J., Readhead, A. C. S., and Unwin, S. C. 1986, *A. J.*, **91**, 494.
- Noordam, J. E., and de Bruyn, A. G. 1982, *Nature*, **299**, 597.
- Olsen, E. T. 1970, *A. J.*, **75**, 764.
- Pearson, T. J., Barthel, P. D., Lawrence, C. R., and Readhead, A. C. R. S. 1986, *Ap. J. (Letters)*, **300**, L25.
- Pearson, T. J., and Readhead, A. C. S. 1984, *Ann. Rev. Astr. Ap.*, **22**, 97.
- Perley, R., Fomalont, E., and Johnston, K. J. 1982, *Ap. J. (Letters)*, **255**, L93.
- Porcas, R. W. 1984, in *IAU Symposium 110, VLBI and Compact Radio Sources*, ed. R. Fanti, K. Kellermann, and G. Setti (Dordrecht: Reidel), p. 157.
- Schilizzi, R. T., and de Bruyn, A. G. 1983, *Nature*, **303**, 26.
- Schmidt, M. 1974, *Ap. J.*, **193**, 505.
- Simon, R. S., Hall, J., Johnston, K. J., Spencer, J. H., Waak, J. A., and Mutel, R. L. 1987, *Ap. J. (Letters)*, submitted.
- Strom, R. G., and Willis, A. G. 1980, *Astr. Ap.*, **85**, 36.
- Ulvestad, J., Johnston, K., Perley, R., and Fomalont, E. 1981, *A. J.*, **86**, 1010.
- Waak, J. A., Spencer, J. H., Johnston, K. J., and Simon, R. S. 1985, *A. J.*, **90**, 1989.
- Walker, R. C. 1984, in *NRAO Workshop 9, Physics of Energy Transport in Extragalactic Radio Sources*, ed. A. H. Bridle and J. A. Eilek (Green Bank, National Radio Astronomy Observatory), p. 20.
- Wardle, J. F. C., and Potash, R. I. 1984, in *NRAO Workshop 9, Physics of Energy Transport in Extragalactic Radio Sources*, ed. A. H. Bridle and J. A. Eilek (Green Bank: National Radio Astronomy Observatory), p. 30.

P. BIERMANN, A. ECKART, C. SCHALINSKI, and A. WITZEL: Max-Planck-Institut für Radioastronomie, Auf dem Hügel 69, D-5300 Bonn 1, Federal Republic of Germany

K. J. JOHNSTON and R. S. SIMON: Code 4130, Radio and Infrared Astronomy Branch, E. O. Hulburt Center for Space Research, Naval Research Laboratory, Washington, DC 20375-5000

R. G. STROM: Netherlands Foundation for Radio Astronomy, Radiosterrenwacht, Dwingeloo, P.O. Box 2, 7990 Dwingeloo, The Netherlands